Proceedings of the
2007 IEEE Intelligent Vehicles Symposium
Istanbul, Turkey, June 13-15, 2007

Compliant MEMS Crash Sensor Designs: The Preliminary Simulation Results

Ümit Sönmez

Abstract: **In this work two new compliant MEMS designs are introduced. The first one is a fully compliant mechanism consist of snap-through buckling arcs. The second one is a compliant bistable mechanism making use of buckling beams. These compliant mechanisms incorporate large deflecting arcs and beams, and a shuttle or a slider. The kinematic simulation of these novel mechanisms are studied using nonlinear Elastica theory, and numerically solving the nonlinear algebraic equations. The large-deflection analysis of the flexible snap-through buckling arc beams and pin-pin buckling beams are utilized using polynomials fits to exact Elastica Solution. The normalized kinematic responses of both mechanisms are investigated. Some of the crash test impact loadings in literature are reviewed in details. The nonlinear equation of motion including the inertia of shuttle, and the stiffness obtained from Elastica theory is simulated for an example pulse impact loading using numerical Runge-Kutta methods for Design I. These compliant MEMS are suitable for crash detections and can be fabricated with the integrated circuit on the same board to be used for Intelligent Safety Systems.**

Word Count: 3518
Key Words: Compliant Mechanisms; MEMS; ITS, ISS, Automotive Crash Sensors; Large Deflection Theory of Flexible Beams; Elastica Theory; Crash Sensor Data, Nonlinear Dynamic Response.

I. INTRODUCTION

Applications of compliant mechanisms have been increasing due to the need of new types of flexible mechanisms [1]. Compliant mechanisms supply their motion with the deflections of their flexible members. The same mechanism would have been a structure if it members were rigid [2]. Reduction in the complexity of the assembly, in the part-count, in the need of lubrication and of the weight can be shown as some of the main reasons why compliant mechanisms are preferred [2-3]. Compliant mechanisms consist of at least one flexible member along with the conventional rigid links. The mobility of the compliant mechanisms is achieved not only due to relative movements of the joints, but also due to relative deflection of the flexible links. A compliant mechanism is called fully or partially compliant depending on the existing of traditional links and joints. A fully compliant mechanism does not require assembly of its parts.

Using traditional rigid links and elastic joints, a compliant mechanism design might be achieved as well as using flexible links and traditional joints. The use of flexible members can make a mechanism comparatively light, which may enhance its use in certain applications.

II. MEMS AND COMPLIANT MEMS

Micro-electro-mechanical systems (MEMS) technology has contributed to the improved performance, reliability and lower-cost sensors that support basic automobile functions within the automotive industry. MEMS technology is expected to play an important role in the future of Research and Development of automotive industry [4]; particularly in the active safety area.

MEMS sensors have the following advantages: they are deterioration-free and are durable for long periods; they have good dynamic characteristics, superior impact resistance, low power consumption, low cost, they are small in size, and easy for installation. MEMS are considered to be as a key technology with potential to meet the requirements of the Intelligent Transportation Technology (ITS). MEMS sensors used in automotive systems etc. usually comprise micro beams and inertial mass formed by etching part of a silicon substrate, and piezo-resistors formed as strain gauges on the beams. Applications of MEMS sensors are not limited to airbag systems. They are also used in vehicle motion control systems, for example in the Antilock Braking System (ABS).

Crash sensors can detect and calculate crash parameters such as velocity and acceleration. Existing technologies for active safety are being modified using MEMS sensors to enhance the performance of current systems; such as airbags or belt pre-tension devices. These systems reduce the risk of injury and its level during a crash which motivates the development of Intelligent Safety Systems (ISS).

In this research two compliant MEMS designs are introduced as shown in Figures 1-2. These mechanisms work on the principle of large deflecting arcs and the beams and achieve motion by the deflection of their members. Prescribed motion profiles can be obtained more easily using buckling members in compliant mechanism design [5]. If these mechanism's members were rigid the mechanism would have zero degree of freedom.

Manuscript received January 22, 2007. This work was supported by the *European Union Framework Program 6* through project *INCO-16426* (AUTOCOM Project).

Ümit Sönmez is with the Mechanical Engineering Department, Istanbul Technical University, Gümüşsuyu İstanbul, 34437, Turkey (e-mail: usonitu@gmail.com).

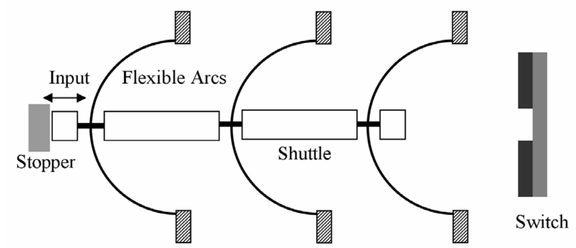

Figure 1: A fully compliant linear displacement mechanism consists of snap-through buckling arcs.

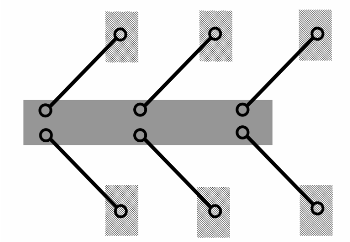

Figure 2: A compliant bistable mechanism design consists of buckling beams.

II. A. COMPLIANT DISPLACEMENT MECHANISM CONSIST OF ARCS

The kinematic response of a flexible arc loaded at its center quasi-staticly is examined and kinematic conditions leading to snap-through and snap-back buckling are discussed. If the arc is pushed by a slowly increasing force, part AB of the load deflection curve would be obtained as shown in Figure 3. At point B, the system (the arc and the shuttle mass) will snap-through to point C. The load at points B and C are the same except they represent different parts of the spring regions (softening part and hardening part). If the applied force is further increased, the region shown by CD would be obtained. If the force is decreased the load deflection points between CE are obtained. As applied load continues to decrease to a minimum (point E) the system snaps back to point F. The load at points E and F are the same but they correspond to different regions of arc deflection. Further decrease in load causes return to the original shape.

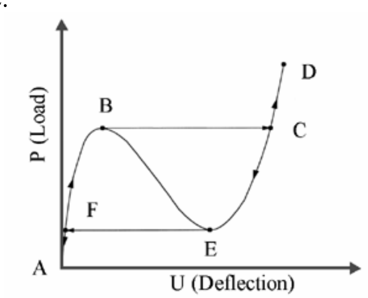

Figure 3: Kinematic response of a flexible arc to an increasing/decreasing load.

II. B. Compliant Bistable Mechanism Design

Compliant bistable mechanisms are gaining popularity since they could be used as MEMS switches, valves and clamps. Howell [2] reserved a chapter in his book, "Compliant Mechanisms" to design and synthesize bistable compliant mechanisms.

Tsay et al. [6] proposed a design of a fully compliant bistable micro-mechanism for the application of switching devices. They adopted the topology of a fully compliant four-bar linkage to synthesize the mechanism. The experimental results confirmed the validity of their theory. Casals-Terre and Shkel [7] explored structural resonance phenomena to switch between two stable positions of a truss-like micro bistable mechanism. They modeled the micro mechanism using a Pseudo Rigid Body Method and illustrated analytically the feasibility of driving the micro mechanism into resonance and achieving dynamical switching. Qui [8] designed and fabricated parallel cosine shaped beams to create bistability. His mechanism does not rely on hinges, and works on snap-through buckling principle of the curved beams, stays stable on the snapped position due to variable thickness of parallel curved beams.

A compliant micro bistable micro mechanism design is introduced in Figure 2. Bistable mechanisms have two stable static equilibrium positions. These mechanisms potential strain energy versus displacement plots exhibit two local minima. Bistable mechanisms could stay in these positions without any support of external forces, in the extent of motion. Therefore if the mechanism is left in these positions they would stay, even they have deflected flexible members. The mechanism shown in Fig. 2 consists of large deflecting initially straight imperfect beams and a slider. The kinematic and dynamic simulation of this compliant micro bistable mechanism might be studied using the presented polynomials *(instead of using Elastica Theory)*, vector loop closure and numerically solving nonlinear equation of motion.

III. LARGE DEFLECTION ANALYSIS OF CURVED BEAMS

The load deflection characteristics of curved beams offer new possibilities as compliant mechanism members and compliant MEMS. Specifically circular arcs loaded vertically at their crown may buckle symmetrically having a snap-through load deflection curve.

Nonlinear analysis of curved beams begins with Euler (1744) who considered rods with initial curvature. Euler's theory is suitable for calculating deflections of slender arcs. In the analytical analysis of high arcs, it is necessary to use exact nonlinear theories. Such arcs buckle symmetrically by snap-through or asymmetrically sideways (for pinned-pinned endpoints) after having large pre-buckling deformations. High circular arcs subjected to a vertical point load applied at their crown may show two different kinds of behavior depending on the boundary conditions (fixed or pinned) and height to span ratio (curved beam angle). These instability types are asymmetric bifurcation (sideways) buckling or symmetric snap-through buckling.

The instability of fixed (clamped) circular arcs was investigated by Schmidt and DaDeppo [9]. They concluded that end constraints of circular arcs greatly affect the type of buckling. While pinned-pinned high rise arcs under critical load buckle by bifurcation, the fixed-fixed arcs buckle symmetrically by snap through for span angles less than 270°.

III. A Snap-Through Buckling of Fixed Circular Arcs Subjected to a Point Load

The original configuration of the curved beam is shown in Figure 4.

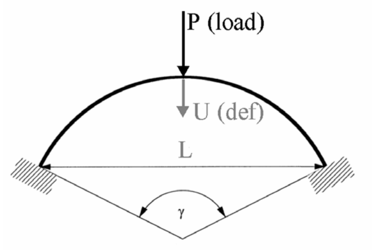

Figure 4: Original configuration of the curved beam

In Figure 4, the arc span is represented by L and the arc angle is γ. A semi-circular arc γ=180º considered for this study. The complete set of the Equations concerning symmetrical deflection of the arc are given in [10, 11], the reader should refer to them for detailed derivation and explanation.

Curve fitting to the normalized load deflection plot of fixed-fixed snap-through buckling arc constraining the correlation coefficient to be $\rho > 0.9998$ has resulted in a 9th order polynomial with a correlation coefficient $\rho = 0.99994$. The polynomial is given by Eq. (1), and the corresponding fit to the exact solution is shown in Figure 5.

$$p_{norm}(u) = \frac{PL^2}{EI} = 87991.906u^9 - 348868.40u^8 + \ldots$$
$$594702.72u^7 - 569172.39u^6 + 336475.73u^5 - \ldots \quad (1)$$
$$127389.26u^4 + 31406.626u^3 - 5359.8993u^2 + \ldots.$$
$$650.55u$$

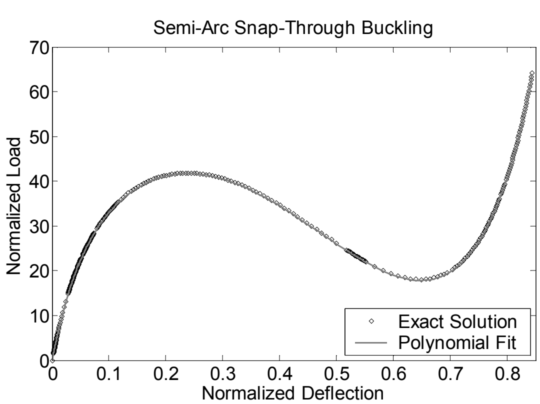

Figure 5: Snap through bucking of the flexible arc. The exact Elastica solution and the corresponding 9th order fit

III. B Large Deflection Analysis of Fix-Free Curve Beam

Nonlinear deflection theory of curved beams is given in [12, 13]. The geometry of the initially circular shaped beams is shown in Figure 6. Under the influence of horizontal P load the beam end undergoes horizontal and vertical deflections (h0-h) and (b0-b) respectively. The load deflection characteristic of a fixed-free beam subjected to a horizontal load is same as that of a pinned-pinned beam shown in Figure 7 due to the symmetry.

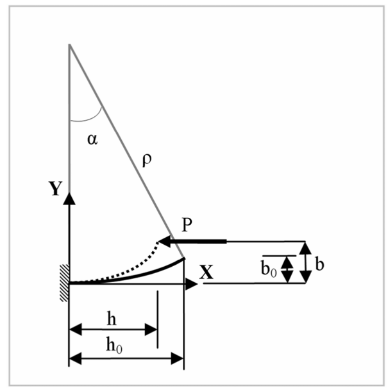

Figure 6: Curved beam subjected to horizontal load.

The forces acting on a simple pinned-pinned segment are collinear along the line between the two pin joints. Pin ends do not carry moments therefore pinned-pinned flexible beam is a two-force member (See figure 7).

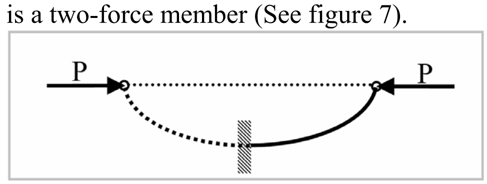

Figure 7: Pin ended curved beam, a two-force member.

Curved beams with α = 0.01 radians considered in section, and it represents and almost straight beam. Deflection solutions are obtained; until the fix-free beam's free end touches to the wall (or pinned ends touch each other). Normalized load ($p=PL^2/EI$) and normalized deflection ($u=y/L$) results are plotted in Figure 8.

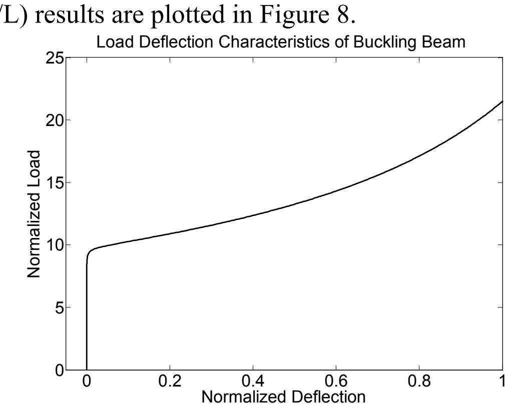

Figure 8: Load deflection characteristics for pin-pin buckling beam

III.C KINEMATIC ANALYSIS OF BISTABLE MECHANISM

The compliant bistable mechanism kinematic diagram is shown in Figure 9. In order to obtain the kinematic response of the mechanism; the loop closure equation and the static equilibrium equations (given below) need to be solved.

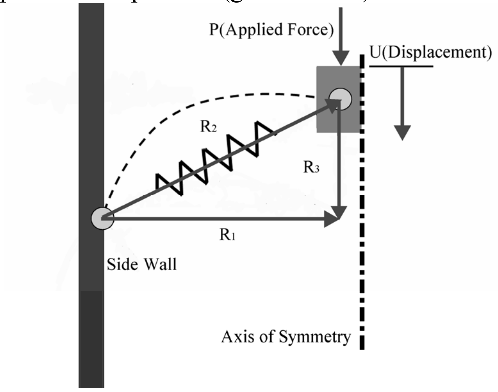

Figure 9: Kinematic Analysis of Design II.

$$V = L_{beam} - \sqrt{(L_{beam}\sin 45° - U)^2 + (L_{beam}\cos 45°)^2} \quad (2)$$

$$\tan\alpha = (L_{beam}\sin 45° - U)/L_{beam}\cos 45° \quad (3)$$

$$F_{applied} = 2NF_{beam}\sin\alpha \quad (4)$$

Where U is the shuttle displacement, V is the buckling beam deflection, α is the R_2 angle with horizontal, N is the pair of side buckling arms, and $F_{applied}$ is the applied force magnitude for the corresponding displacement. Initial dome angle of bucking beams are taken 45º in this investigation. Solving above equations using a nonlinear algebraic solution routine gives the following normalized load deflection plot (see Figure 10).

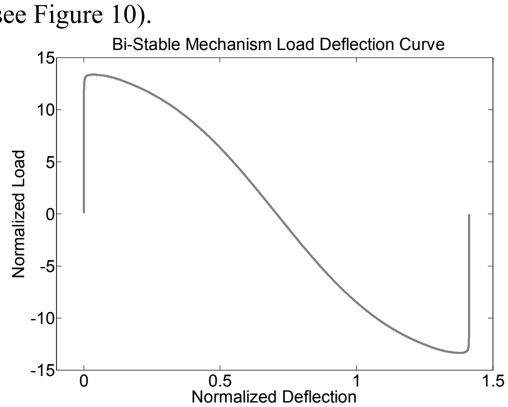

Figure 10: Normalized load deflection characteristics of the proposed bistable mechanism.

Because of load-deflection characteristics; polynomial functions are not suitable to be fit to this graph; this leads to use of rationale functions. Fitting with a good degree of accuracy resulted in 5th degree of rationales represented by Eq. (5) and given in Table 1. This fit represents until the shuttle cross the zero load condition (the positive part of the curve), for complete functional representation, the point wise symmetry about the zero crossing needs to be considered.

$$p(u) = \frac{PL^2}{EI} = \frac{p_1u^4 + p_2u^3 + p_3u^2 + p_4u + p_5}{u^5 + q_1u^4 + q_2u^3 + q_3u^2 + q_4u + q_5} \quad (5)$$

Coefficients	Value	Coefficients	Value
p1	-21.38	**q1**	-1.409
p2	14.84	**q2**	1.174
p3	-0.1731	**q3**	-0.0174
p4	0.265	**q4**	0.01984
p5	$1.55*10^{-7}$	**q5**	$2.588*10^{-6}$

Table 1: Curve fit results for bistable mechanism.

IV. CRASH DATA LITERATURE SURVEY

Four papers were reviewed in details to gather the crash data experimental results in this section. The same data are planned to be used in future studies for the design methodologies of both mechanisms considering different crash detection limits.

General Motors (GM) vehicles with airbag protection [14] have recorded airbag status and crash severity data for impacts causing a deployment. The new vehicles (since 1994) were equipped with an analog accelerometer and a computer algorithm integrated in a Sensing and Diagnostic Module (SDM). In order to provide the estimate of crash severity the SDM computed and stored the change in longitudinal vehicle velocity (ΔV) during the impact (see figure 11). The SDM algorithm is activated when two successive samples exceed about 2 g's of deceleration. The SDM computes ΔV by integrating the average acceleration samples and stores them. The crash pulse can be represented by a low frequency velocity change data (ΔV).

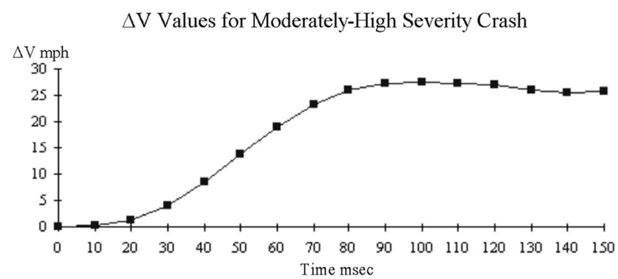

Figure 11: Post-impact ΔV vs. time Ref [14]

Figure 11 shows the ΔV values for a representative moderately-high severity crash. The typical ΔV increases smoothly until it levels off at approximately 70-120 msec and is usually at least 12 mph in magnitude. This is in agreement with the design goal of deploying the airbags. The longitudinal vehicle velocity is expected to exceed 9-14 mph when a fixed barrier impact happens. However, the history of recorded deployments was typically a short duration event (20 msec or less) with a total velocity change of less than 7 mph. These false deployments were produced by small rocks or debris striking the underside of the vehicle with high impulsive energy.

The attainment of advanced regulations for side impact crash tests requires an improved and faster detection method as presented in [15]. Therefore the sensor has to able to recognize the severe ness of an accident within a short time having a high confidence level. The output signals represented by pressure sensors and by acceleration sensors during a side crash impact are presented in Figure 12 [15]. In each case two events are regarded: First an impact is present, therefore the safety systems must be activated. Second an innocent impact, (e.g. an impact of a ball is present) is present therefore the safety systems may not be activated.

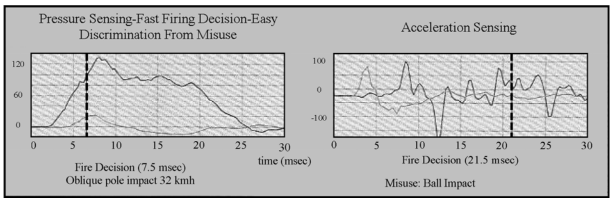

Figure 12: Pressure sensor signals compared with acceleration sensors Ref [15]

Figure 12 shows the advantages of the pressure sensors.

- The first one is the reliable decision to activate the safety systems faster.
- The second one is substantially easier to differ between material accident and insignificant impulses.

Passenger response variability was measured and recorded [16] using a Bio-RID dummy to rear-end collisions in 20 different vehicles. The objective of their study (Siegmund et. al., 2005) was to quantify the passenger response variability due to differences in vehicle and seat design, in low-speed rear-end collisions. Vehicles were rolled backwards into a rigid barrier at 8 km/h and the dynamic responses of the vehicle and the dummy were recorded (see Figure 13).

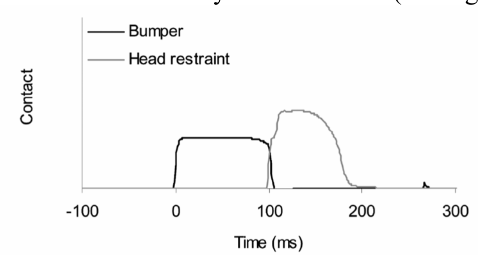

Figure 13: Bumper and head restraint sample data for 8 km/h impact Ref [16]

A series of 49 km/h sled crash tests [17] were performed using the Hybrid III 6-year-old dummy for three seating adjustments. All crash tests were conducted at a 49 km/h impact speed with the acceleration pulses shown in Figure 14. The speed, the maximum acceleration, and the duration are similar to the FMVSS 213 acceleration pulse, "the current iteration of Federal Motor Vehicle Safety Standard FMVSS 213 Child Restraint Systems (Code of US Federal Regulations, 1999)".

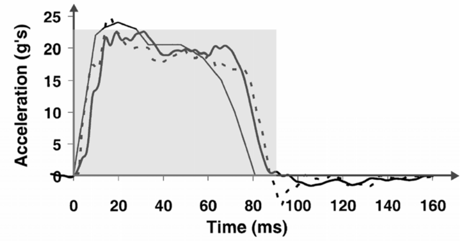

Figure 14: Sled crash acceleration pulses (nearly rectangular) Ref [17]

V. Dynamic Response

The proposed mechanisms have 1 D.O.F therefore it can be modeled with a classic lumped mass, damper, and spring system (see Figure 15). The lumped system stiffness' are represented by a polynomial fit to exact solution (its Elastica equivalent function).

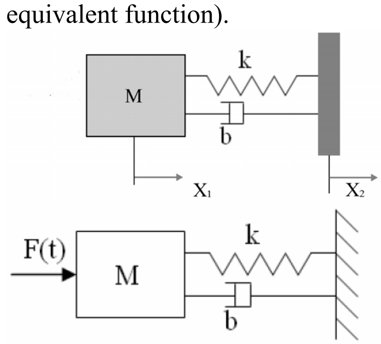

Figure 15: Mass, damper, and spring systems
a) Suitable for a sensor input
b) Suitable for an applied force response

The Figure 15 shows two lumped models of proposed mechanisms. The first one is suitable for sensor simulation where the input comes from base excitement as crash acceleration, velocity and displacement. The second one is suitable to obtain the design response to various types of loading condition which could give system's non-linear frequency response etc. The equation of motion of the lumped system shown in Figure 15.b is as follows;

$$M\ddot{x}+C\dot{x}+K(x+ax^2+bx^3+...)=F(t) \quad (5)$$

The normalized nonlinear spring stiffness is represented by a polynomial fit in Eq. (1) can be used to obtain the nonlinear spring rate of the micro bistable mechanism (example mechanism I) using the following formula.

$$U = uL$$

$$P=\frac{EI}{L^2}\left[a_9(U/L)^9+..+a_1(U/L)\right] \quad (6)$$

The example mechanism I dimensions and material properties is given Table 2.

Mechanism Part	**Dimensions or Mechanism Properties**

Number of Arcs	1
Arc Beam Span	L = 200 micron
Rigid Coupler Mass	20.5 micro-gram
Arc Cross Section Dimensions	Out of plane width 3.5 µm In plane thickness 2.0 µm
$I=bh^3/12$	$2.33*10^{-24}$ m^4
Damping Coefficient	C=0.001 N*s/m
E (Elasticity Modulus)	$1.65*10^{11}$ N/m^2

Table 2: Design I dimensional and structural properties

In order to see the dynamic response of the bistable mechanism, a step input with the magnitude $1.1*P_{buckling}$ is applied to the Design I at 100 msec, for a duration of 100 msec; this is consistent with data in [17]. The tip deflection (slider position) versus time is plotted in Figure 16 which shows that the response for snap-through is less than 10 msec which is suitable for fast detection.

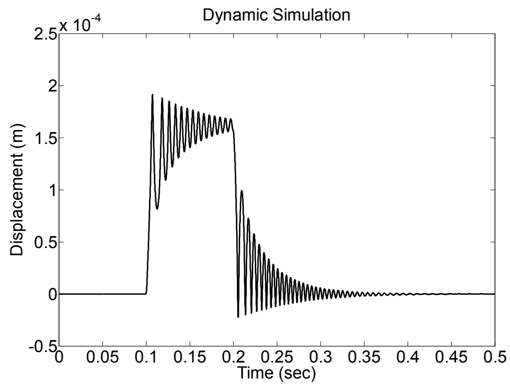

Figure 16: Dynamic Response of Example I

The phase diagram of Design I (see Figure 17) shows that; there are two attractors one is at the original configuration and the other one is at the snap through position where the switch is activated.

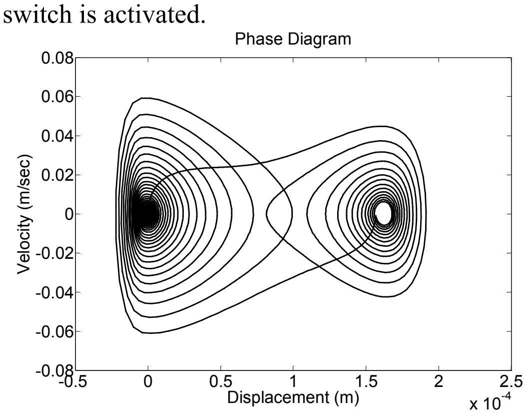

Figure 17: Phase response of Example I

VI. Discussion And Conclusions

This paper presents an introduction to two novel compliant crash sensor designs. These compliant MEMS designs are expected to lower the cost of the crash sensors. The kinematic analysis of both sensors is presented and the dynamic simulation example of the first design subject to a pulse force is studied.

The detailed dimensional design methodologies of both complaint MEMS needs to be done considering falsifying impact inputs and sending the signal when the real impact is present in Future studies. More than one design architecture or combination of several introduced micro designs side by side might be used to determine the severity of the impact. For example: One compliant MEMS can be design to activate the switch for the crash acceleration range 10 g's and crash time less than 20 msec. and the other one the crash acceleration range 50 g's and time greater than 100 msec etc. The complete dynamic design methodology and electronic IC units of these sensors are planned for near future studies.

References

[1] Sönmez, Ü., 2007, "Introduction to Compliant Long Dwell Mechanism Designs Using Buckling Beams and Arcs", ASME J. Mech. Des., Article in Press.

[2] Howell, L.L., 2001, "Compliant Mechanisms", 1st edition John Wiley & Sons, Inc., New York.

[3] Vogel, S., 1995, "Better Bent than Broken," Discover, May 1995, pp. 62-67.

[4] Y. Ueno, and N. Kawahara, "Micro-system Technologies for Automotive Applications", pp. 21-27.

[5] Compliant Mechanism Design and Synthesis Using Buckling and Snap Through Buckling of Flexible Members, Ph.D. Thesis, The Pennsylvania State University, December 2000. State College Pennsylvania.

[6] Tsay J., Su L. Q and Sung C. K., "Design of a Linear Micro-Feeding System Featuring Bistable Mechanisms." Journal of Micromechanics and Micro-engineering. Vol. 15 (2005) pp. 63–70.

[7] Casals-Terre, J., and Shkel A., 2004, "Dynamic Analysis of a Snap-Action Micro-mechanism", Proceedings of IEEE Conference, pp. 1245-1248.

[8] Qiu, J., Lang, J.H., and Slocum, H., 2004, "A Curved-Beam Bistable Mechanism", Journal Of Micro-electromechanical Systems, Vol. 13, No. 2, pp. 137-146.

[9] DaDeppo, D.A. and Schmidt, R., "Nonlinear Analysis of Buckling and Postbuckling Behavior of Circular Arches," Zeitschrift fur angewandte Mathematik und Physik, Vol. 20, No. 6, 1969, pp. 847-857.

[10] Nordgren, R. P., "On Finite Deflection of an Extensible Circular Ring Segment," International Journal of Solids and Structures, Vol. 2, No.2, April. 1966, pp. 223-233.

[11] Frisch-Fay, R., Flexible Bars, Butterworth & Co. (Publishers) Limited, London, 1962.

[12] Conway H. D., 1956, 'The Nonlinear Bending of Thin Circular Rods', Journal of Applied Mechanics, 23, 7-10.

[13] Sathyamoorty M., Nonlinear Analysis of Structures, (Sec. 4.2), CRC Press, New York, 1998.

[14] A. Chidester, J. Hinch, T. C. Mercer, and K. S. Schultz, "Recording Automotive Crash Event Data" International Symposium on Transportation Recorders, May 1999.

[15] M. Brauer, and K. Krupka, "Advanced Pressure Sensors with High Flexibility for Side Crash Detection", Safety, pp. 45-51.

[16] G. P. Siegmund, B. E. Heinrichs, D. D. Chimich, and J. Lawrence, "Variability in Vehicle and Dummy Responses in Rear-End Collisions", Traffic Injury Prevention, Taylor & Francis Inc, vol 6: pp. 267–277, 2005.

[17] C. P. Sherwood, C. G. Shaw, L. Van Rooij, R.W. Kent, J. R. Crandall, K. M. Orzechowski, M. R. Eichelberger, and D. Kallieris, "Prediction of Cervical Spine Injury Risk for the 6-Year-Old Child in Frontal Crashes", Traffic Injury Prevention, 2003, vol 4, pp. 206–213.", Safety pp. 115-127.